Coordinated beating of algal flagella is mediated by basal coupling

Kirsty Y. Wan[a] and Raymond E. Goldstein[a,1]

[a]Department of Applied Mathematics and Theoretical Physics, University of Cambridge, Cambridge CB3 0WA, United Kingdom

Edited by Peter Lenz, Philipps University of Marburg, Marburg, Germany, and accepted by the Editorial Board March 14, 2016 (received for review September 30, 2015)

Cilia and flagella often exhibit synchronized behavior; this includes phase locking, as seen in *Chlamydomonas*, and metachronal wave formation in the respiratory cilia of higher organisms. Since the observations by Gray and Rothschild of phase synchrony of nearby swimming spermatozoa, it has been a working hypothesis that synchrony arises from hydrodynamic interactions between beating filaments. Recent work on the dynamics of physically separated pairs of flagella isolated from the multicellular alga *Volvox* has shown that hydrodynamic coupling alone is sufficient to produce synchrony. However, the situation is more complex in unicellular organisms bearing few flagella. We show that flagella of *Chlamydomonas* mutants deficient in filamentary connections between basal bodies display markedly different synchronization from the wild type. We perform micromanipulation on configurations of flagella and conclude that a mechanism, internal to the cell, must provide an additional flagellar coupling. In naturally occurring species with 4, 8, or even 16 flagella, we find diverse symmetries of basal body positioning and of the flagellar apparatus that are coincident with specific gaits of flagellar actuation, suggesting that it is a competition between intracellular coupling and hydrodynamic interactions that ultimately determines the precise form of flagellar coordination in unicellular algae.

green algae | flagella | synchronization | basal fibers | internal coupling

Possession of multiple cilia and flagella bestows significant evolutionary advantage upon living organisms only if these organelles can achieve coordination. This may be for purposes of swimming (1, 2), feeding (3), or fluid transport (4, 5). Multiciliation may have evolved first in single-celled microorganisms due to the propensity for hydrodynamic interactions to couple their motions, but it was retained in higher organisms, occurring in such places as the murine brain (6) or human airway epithelia (7). Since Sir James Gray first noted that "automatic units" of flagella beat in "an orderly sequence" when placed side by side (8), others have observed the tendency for nearby sperm cells to undulate in unison or aggregate (9, 10), and subsequently the possible hydrodynamic origins of this phenomenon have been the subject of extensive theoretical analyses (2, 5, 11). Despite this, the exclusiveness and universality of hydrodynamic effects in the coordination of neighboring cilia and flagella remains unclear.

We begin by considering one context in which hydrodynamic interactions are sufficient for synchrony (12). The alga *Volvox carteri* (VC) is perhaps the smallest colonial organism to exhibit cellular division of labor (13). Adult spheroids possess two cell types: Large germ cells interior of an extracellular matrix grow to form new colonies, whereas smaller somatic cells form a dense surface covering of flagella protruding into the medium, enabling swimming. These flagella generate waves of propulsion, which, despite lack of centralized or neuronal control ("coxless"), are coherent over the span of the organism (14). In addition, somatic cells isolated from their embedding colonies (Fig. 1*A*) beat their flagella in synchrony when held sufficiently close to each other (12). Pairwise configurations of these flagella tend to synchronize in phase (IP) when oriented with power strokes in the same direction, but antiphase (AP) when oriented in opposite directions, as predicted (15) if their mutual interaction were hydrodynamic. However, not all flagellar coordination observed in unicellular organisms can be explained thus. The lineage to which *Volvox* belongs includes the common ancestor of the alga *Chlamydomonas reinhardtii* (CR) (Fig. 1*B*), which swims with a familiar IP breaststroke with twin flagella that are developmentally positioned to beat in opposite directions (Fig. 1 *C* and *D*). However, a *Chlamydomonas* mutant with dysfunctional phototaxis switches stochastically the actuation of its flagella between IP and AP modes (15, 16). These observations led us to conjecture (15) that a mechanism, internal to the cell, must function to overcome hydrodynamic effects.

Pairs of interacting flagella evoke no image more potent than Huygens' clocks (17): Two oscillating pendula may tend toward synchrony (or antisynchrony) if attached to a common support, whose flexibility provides the necessary coupling. Here we present a diverse body of evidence for the existence of a biophysical equivalent to this mechanical coupling, which, in CR and related algae, we propose is provided ultrastructurally by prominent fibers connecting pairs of basal bodies (BB) (18) that are known to have contractile properties. Such filamentary connections are absent in configurations of two pipette-held uniflagellate cells and defective in a class of CR mutants known as *vfl* (variable number of flagella) (Fig. 1*B*). We show, in both cases, that the synchronization states are markedly different from the wild-type breaststroke.

Seeking evidence for the generality of putative internal control of flagellar coupling in algal unicells, we use light microscopy, high-speed imaging, and image processing to elucidate the remarkable coordination strategies adopted by quadriflagellates, octoflagellates, and hexadecaflagellates, which possess networks of basal, interflagellar linkages that increase in complexity with flagella number. The flagellar apparatus, comprising BBs, connecting

Significance

In areas as diverse as developmental biology, physiology, and biomimetics, there is great interest in understanding the mechanisms by which active hair-like cellular appendages known as flagella or cilia are brought into coordinated motion. The prevailing theoretical hypothesis over many years is that fluid flows driven by beating flagella provide the coupling that leads to synchronization, but this is surprisingly inconsistent with certain experimentally observed phenomena. Here we demonstrate the insufficiency of hydrodynamic coupling in an evolutionarily significant range of unicellular algal species bearing multiple flagella, and suggest that the key additional ingredient for precise coordination of flagellar beating is provided by contractile fibers of the basal apparatus.

Author contributions: K.Y.W. and R.E.G. designed research, performed research, analyzed data, and wrote the paper.

The authors declare no conflict of interest.

This article is a PNAS Direct Submission. P.L. is a guest editor invited by the Editorial Board.

Freely available online through the PNAS open access option.

[1]To whom correspondence should be addressed. Email: R.E.Goldstein@damtp.cam.ac.uk.

This article contains supporting information online at www.pnas.org/lookup/suppl/doi:10.1073/pnas.1518527113/-/DCSupplemental.

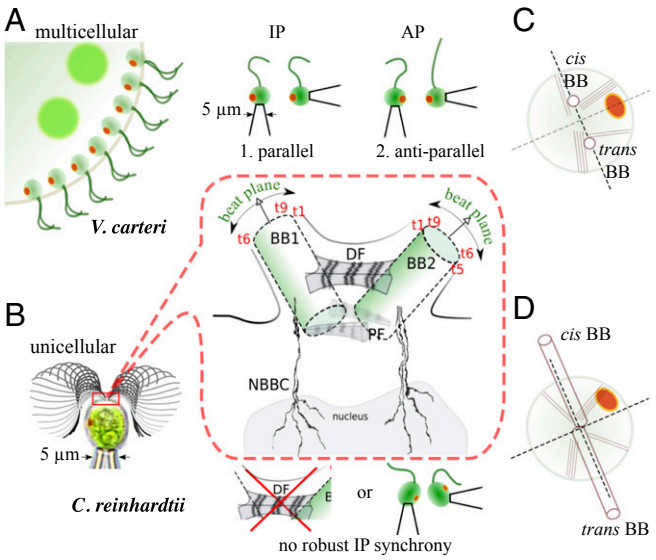

Fig. 1. Flagellar synchronization in multicellular vs. unicellular algae. (*A*) Pairs of isolated, somatic flagella of VC tend to synchronize either in IP or AP depending on their relative orientation. (*B*) CR flagella maintain position 2 yet swim a robust IP breaststroke that is lost (*i*) by mutation of the DF, and (*ii*) in pairs of nearby uniflagellate cells. (*C* and *D*) Ultrastructure comprising BBs, rootlets, and eyespot in VC (*C*) and CR (*D*). Numbered microtubule triplets are denoted by t1–t9.

fibers, microtubular rootlets, and the transition regions of axonemes, is among the most biochemically and morphologically complex structures occurring in eukaryotic flagellates (19). The significance of basal coupling relative to hydrodynamics is highlighted, especially in maintaining relative synchrony in diametrically opposed pairs of flagella. Our study reconciles species-specific swimming gaits across distinct genera of green algae with the geometry of flagellar placement and symmetries of their differing basal architecture—so often a key phylogenetic character (20).

Although many features of eukaryotic flagellar axonemes are conserved from algae to mammals [e.g., composition by microtubules, motive force generation by dyneins, signal transduction by radial spokes/central pair (16)], far greater diversity exists in the coordination of multiple flagella. Such strategies are vital not only in microswimmers bearing few flagella but also in ciliary arrays. In mice, defects in structures known as basal feet can cause ciliopathies (21), whereas the striated (kinetodesmal) fibers in *Tetrahymena* help maintain BB orientation and resist hydrodynamic stresses (22). Insights from primitive flagellates may thus have significant broader implications.

Results

Synchronization of *Chlamydomonas* Flagella. The basic configuration of two flagella appears in multiple lineages by convergent evolution, e.g., in the naked green alga *Spermatozopsis* (23), in gametes of the seaweed *Ulva* (24), and in swarm cells of *Myxomycetes* (25). CR exemplifies the isokont condition. Cells ovoid, ∼5 μm radius, have flagella ∼1.5× body length and distinguishable by BB age. During cell division, each daughter retains one BB from the mother (26), which becomes associated with the *trans*-flagellum, and a second is assembled localizing near the eyespot and associates with the *cis*-flagellum (Fig. 1 *B* and *D*). When both flagella prescribe identical beats, a nearly planar breaststroke results, which is highly recurrent and stable to perturbations (27). However, despite extensive research (28–32), exactly how this IP breaststroke is achieved has remained elusive; coupling of the flagella pair may be by (*i*) hydrodynamics, (*ii*) drag-based feedback due to cell body rocking, or (*iii*) intracellular means.

CR cells turn by modulation of bilateral symmetry. During phototaxis (33), photons incident on the eyespot activate voltage-gated calcium channels, which alter levels of intracellular calcium, leading to differential flagellar responses. Ionic fluctuations (e.g., Ca^{2+}) alter not only the flagellar beat but also the synchrony of a pair. Gait changes involving transient loss of synchrony (called "slips") occur stochastically at rates sensitive to such environmental factors (15, 27, 34) as temperature, light, chemicals, hydrodynamics, and age of cell culture. In free-swimming cells, slips can alter the balance of hydrodynamic drag on the cell body, producing a rocking motion that promotes subsequent resynchrony of flagella (31), but this does not explain the robust IP synchrony in cells held immobilized on micropipettes (16, 29), nor the motility of isolated and reactivated flagellar apparatuses (35). The altered beat during slips is analogous to the freestyle gait (AP in Fig. 1) characterized in the phototaxis mutant *ptx1*, which stochastically transitions between IP and AP gaits (15, 16). The dependence of CR flagellar synchronization state on physiology through temperature or ionic content of the medium (27) leads us now to the possibility for intracellular coupling of flagella.

Early work (18) identified thick fibers connecting the two *Chlamydomonas* BBs, including a $300\times250\times75$ nm^3 bilaterally symmetric distal fiber (DF), bearing complex striation patterns with a periodicity of ∼80 nm (Fig. 1*B*). Two or more parallel proximal fibers (PF) also connect the BB at one end (Fig. 1*B*). Striation periodicity varies across species, and is changeable by chemical stimuli—indicating active contractility (36). The DF contains centrin, also found in nuclear basal body connectors (NBBCs) (Fig. 1*B*), which are involved in localization of BBs during cell division (37). The two BBs have an identical structure of nine triplet microtubules that form a cartwheel arrangement (38). Importantly, the DF lies in the plane of flagellar beating, and furthermore attaches to each BB at the same site relative to the beating direction of the corresponding flagellum (Fig. 1*B*). This inherent rotational symmetry makes the DF uniquely suited to coordinating the IP *Chlamydomonas* breaststroke.

Hypothesizing a key role for the DF in CR flagellar synchrony, we assess the motility of the mutant *vfl3* (CC1686; Chlamydomonas Center), with DFs missing, misaligned, or incomplete in a large fraction of cells (36). Swimming is impaired: many cells rotate in place at the chamber bottom. In *vfl3*, the number of flagella (0–5), their orientation and localization on the cell body, and cell size are abnormal. BBs still occur in pairs, but not every BB will nucleate a flagellum (39), thus allowing the flagella number to be odd. However, no structural or behavioral defects were observed in the flagella (36).

A number of representative configurations of flagella occur in *vfl3*, for cells bearing two or three flagella (Fig. 2 *A*–*F*). Fig. 2*G* presents the wild-type case. We consider pairwise interactions between flagella. For each flagellum, we extract a phase $\phi(t)$ from the high-speed imaging data by interpolating peaks in the SD of pixel intensities measured across predefined regions of interest. The *vfl3* flagellar beating frequencies are found to be more variable than the wild type, so we elect to determine phase synchrony between pairs of flagella via a stroboscopic approach. Given phases ϕ_1, ϕ_2, we wish to characterize the distribution $\mathcal{P}_C(\chi)$ of $\chi=\phi_2 \bmod 2\pi|_{t:\phi_1 \bmod 2\pi=C}$. Thus, the phase of flagellum 2 is measured conditional on the phase of flagellum 1 attaining the value C. From long timeseries, we determine χ by binning $[0,2\pi]$ into 25 equiphase intervals centered around $\{C_k, k=1,\ldots,25\}$ to obtain the N_k corresponding time points for which $\phi_1 \bmod 2\pi$ falls into the kth interval. The distribution of this conditional phase $\chi^k:=\{\phi_2(t_i), i=1,\ldots,N_k\}$, which is peaked when oscillators phase lock and uniform when unsynchronized, can then be displayed on a circular plot by conversion to a color map. In Fig. 2, we take $k=1$. Phase vectors can be summed and averaged to define a synchronization index

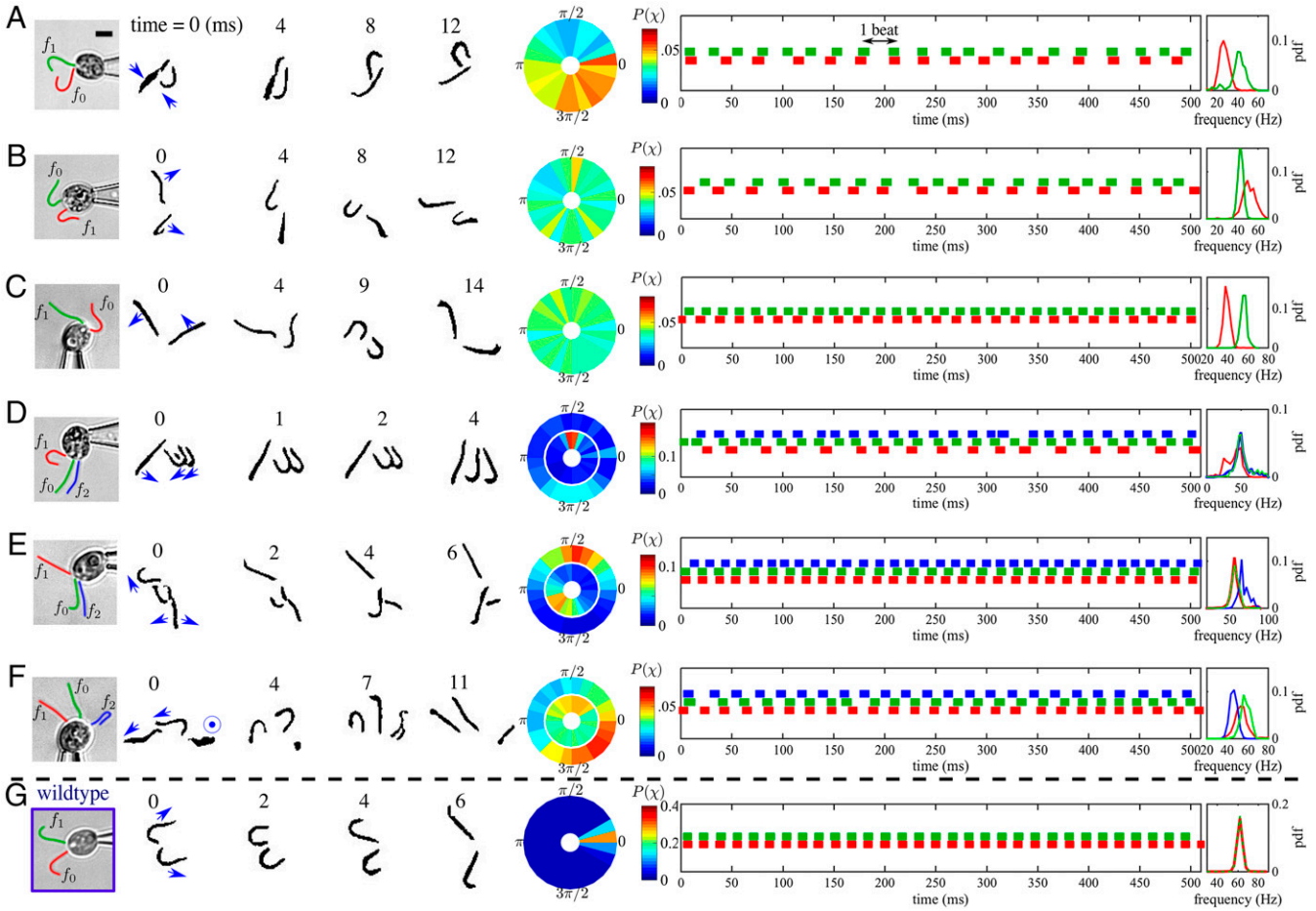

Fig. 2. The CR mutant *vfl3* has defective DF, with abnormal flagella number and orientation. Shown are groups of two or three flagella in orientations of interest. (Scale bar: 5 μm.) (*A* and *B*) Toward or away-facing and flagella-like, i.e., antiparallel; (*C*) cilia-like, i.e., parallel; (*D* and *E*) exhibiting clear hydrodynamic phase locking of closely separated parallel or antiparallel pairs of flagella. Only *F* has a nonplanar aspect: Flagellum f_2 points out of the page. Power stroke directions are indicated by the arrows. Phase distributions $\mathcal{P}_0(\chi)$ of flagellum $f_{1,(2)}$ conditional on the phase of flagellum f_0 are shown on circular plots (in *D*–*F*: f_1 for the inner ring and f_2 for the outer). For *A*–*C*, $S_{1,0} = 0.20, 0.04, 0.04$, and, for *D*–*F*, $(S_{1,0}, S_{2,0}) = (0.30, 0.49), (0.53, 0.40), (0.02, 0.01)$. (*G*) In contrast, for the wild type, $S_{1,0} = 0.96$. Discretized phases are plotted as "footprints" with length proportional to beat cycle duration, with probability density functions of beat frequencies.

$$\mathcal{S} = \frac{1}{25}\sum_{k}^{25}\left|\frac{1}{N_k}\sum_{j}^{N_k}\exp\left(i\chi_j^k\right)\right|, \qquad [1]$$

where $\mathcal{S}_k = 1$ (perfect synchrony) and $\mathcal{S}_k = 0$ (no synchronization).

In *vfl3*, steric interactions between nearby flagella (e.g., Fig. 2*A*) can lead to intermittent beating and reduction in beat frequency. Even when measured beat frequencies differ for flagella on the same cell, periods of phase locking are observed, which we attribute to hydrodynamic interactions (12, 15, 40) (see also Movie S1). In the triflagellates of Fig. 2 *D* and *E*, beating of a given flagella pair becomes strongly coupled, with IP or, respectively, AP synchrony being preferred when flagella are oriented with power strokes parallel or, respectively, antiparallel (compare f_0, f_2 in Fig. 2*D* with f_0, f_2 in Fig. 2*E*). Even biflagellate *vfl3* cells with a native CR-like configuration cannot perform IP breaststrokes (e.g., Fig. 2*B*). In contrast, wild-type CR flagella operating over a large frequency range are able to achieve robust synchrony, despite intrinsic *cis*/*trans* frequency differences of up to 30% during slips, or conditions of physiological stress such as deflagellation (16). Thus, possession of functional or complete DFs appears necessary for CR flagellar synchrony.

Micromanipulation of Flagellate Algae. Next we ask whether the CR breaststroke can instead be produced by hydrodynamic interactions. Use of flagella belonging to different cells offers a tractable alternative to removal by mutation of such physical connectors as the DF. We construct, by micromanipulation, configurations of two flagella that cannot be coupled other than through the immersing fluid.

In Fig. 3*A*, one flagellum was removed from each of two wild-type CR cells by careful mechanical shearing (*Materials and Methods*), so that a CR-like arrangement comprising one *cis* and one *trans* flagellum is assembled. Despite similarity with the wild-type configuration, no sustained IP breaststrokes were obtained. Closely separated (<5 μm) pairs exhibit periods of phase locking. Beat frequencies of these flagella are found to be noisier than their counterparts in intact CR cells, and, consequently, measured phase locking is not robust ($S = 0.08$). The conditional (stroboscopic) phase χ (Fig. 3*A*) is peaked weakly about π, indicating a tendency for AP synchronization, but the IP state is also possible. This bistability is not species-specific; we rendered uniflagellate (see also ref. 12) pairs of pipette-held VC somatic cells (normally biflagellate) and placed them in a similar configuration (Fig. 3*B*). Analysis of the resulting pairwise flagellar interactions indicates a strong preference for AP synchronization, although the IP is again observed (see Movies S2 and S3). Accordingly, the phase stroboscope is now strongly peaked near $\chi = \pi$ (with $S = 0.67$).

The existence, stability, and frequency of IP and AP states are wholly consistent with a basic theory (40) that models a pair of

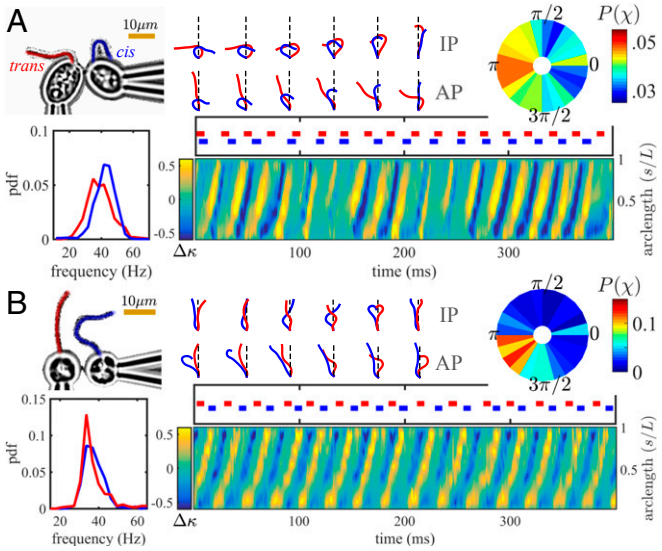

Fig. 3. Coupling (*A*) two CR flagella (one *cis*, one *trans*) and (*B*) two uniflagellated VC somatic cells, both in antiparallel configuration. In both cases, IP and AP states are observed, the AP being preferred. In *B*, hydrodynamic coupling is notably stronger. The pairwise curvature difference $\Delta\kappa$ (per micrometer), plotted on the same time axis as phase footprints, shows propagating high-curvature bends that are coincident during IP, or alternating during AP.

hydrodynamically coupled flagella as beads rotating on springs with compliant radii R separated by distance ℓ (see *SI Appendix*). Assuming $R \ll \ell$, either IP or AP states of synchrony are predicted to be stable depending on whether the beads are corotating or respectively counterrotating (15, 40). Thus, CR-like configurations should tend to AP synchrony. However, in our experiments, flagella often come into such close proximity during certain phases of their beat cycles that the far-field assumptions of the original model break down. Nonlocal hydrodynamic interactions between different portions of flagella must now be considered for the true flagellar geometry (rather than in a phase-reduced bead model). In particular, undulating filaments can be driven by fluid–structure interactions into either IP or AP oscillating modes, depending on initial relative phase (41). The inherent stochasticity of flagellar beating (27) thus leads to transitions between IP and AP states (Fig. 3). Hydrodynamic effects are notably stronger in the case of VC than CR, due to reduced screening by a smaller cell body and a distinctive upward tilt of the flagellar beat envelope. During evolution to multicellularity, this latter adjustment of BB orientation (Figs. 1 *C* and *D*) facilitates beating of flagella confined within a spherical colony. The CR mutant *ptx1* also displays noisy transitions between IP and AP gaits (15) due to an unknown mutation; the implications of this we shall return to later (see *Discussion*).

The similarity of two flagellar waveforms in any given state (IP or AP) can be compared. For ease of visualization, waveforms discretized at equidistant points are ordered from base to tip: $\mathbf{f}_i^{\mathrm{L}}$, $\mathbf{f}_i^{\mathrm{R}}$ for $i = 1, \ldots N_p$, and rescaled to uniform total length. These are rotated by $\mathcal{T}(\alpha)$ through angle α between the horizontal and line of offset between the BBs. We denote by $\mathbf{f}^{\mathrm{L}} \to \mathbf{f}'^{\mathrm{L}} = \mathcal{T}(\mathbf{f}^{\mathrm{L}} - \mathbf{m})$ and $\mathbf{f}^{\mathrm{R}} \to \mathbf{f}'^{\mathrm{R}} = \mathcal{T}(\mathbf{f}^{\mathrm{R}} - \mathbf{m})$, with $\mathbf{m} = (\mathbf{f}_1^{\mathrm{L}} + \mathbf{f}_1^{\mathrm{R}})/2$, and compare the resulting shape symmetries during IP and AP states (Fig. 3 *A* and *B*, stacked). The synchronization index of Eq. **1**, although suitable for identifying presence or absence of phase synchrony, does not discriminate between AP and IP states. Instead, we compute the pairwise curvature difference $\Delta\kappa(t,s) = \kappa_L - \kappa_R$ as a function of time (t) and normalized arclength (s), where κ_L, κ_R are signed curvatures for the left and right flagellum according to their respective power stroke directions. During IP and AP synchrony, $\Delta\kappa$ exhibits a wave pattern at the common or phase-locked frequency. Principal or high-curvature bends propagate from flagellum base to tip in accordance with the mechanism of flagellar beating in these species (0.897 ± 0.213 mm/s for CR, and 0.914 ± 0.207 mm/s for VC). In summary, we have established, in two species, that robust IP synchrony akin to the CR breaststroke does not arise from hydrodynamic coupling between two coplanarly beating flagella arranged in a CR-like configuration, even when beat frequencies are comparable.

Moreover, the propensity for algal flagella to be deformable by hydrodynamic loading (12), e.g., flows generated by nearby flagella, suggests that an internal coupling must be present to compensate in such cases where fluid interactions are contrary to the desired mode of propulsion by flagella in the organism. Given this delicate interplay, will a dramatic perturbation to the state of hydrodynamic interactions between flagella affect their native mode of coordination? For this, we require an organism with more than two flagella. *Tetraselmis* is a thecate quadriflagellate, and is amenable to micromanipulation. Fig. 4*A* depicts a pipette-immobilized *Tetraselmis* cell with flagella free to beat in a pattern qualitatively similar to free-swimming cells observed under identical conditions (see Movie S4), in which flagella maintain a transverse gallop (Figs. 4*C* and 6*D*). One flagellum was then trapped inside a second pipette with suction so as to completely stall its beating, with minimal disruption to the cell. Flagellar dynamics were monitored and interflagellar correlation functions were computed (Fig. 4*B*), showing that the prior beat patterns continue (Fig. 4*C*). The small increase in beat frequency in the remaining flagella ($\sim 5\%$) is consistent with calcium-induced frequency elevation by mechanosensation. This remarkable ability of the cell to sustain its coordination pattern strongly implicates internal beat modulation.

Symmetries of the Algal Flagellar Apparatus. Such a hypothesis brings us now to further detailed study of a large number of lesser-known species that have differing or more complex basal architectures and which, in turn, we find to display varied and novel flagellar coordination strategies. Although it is believed that volvocine green algae (including VC) derived from *Chlamydomonas*-like ancestors, the general classification of Viridiplanta (green plants) has undergone repeated revisions due to the enormous variability that exists in the form and structure exhibited by its member species. Features, both developmental (mitosis, cytokinesis) and morphological (number, structure, arrangement of flagella, nature of body coverings such

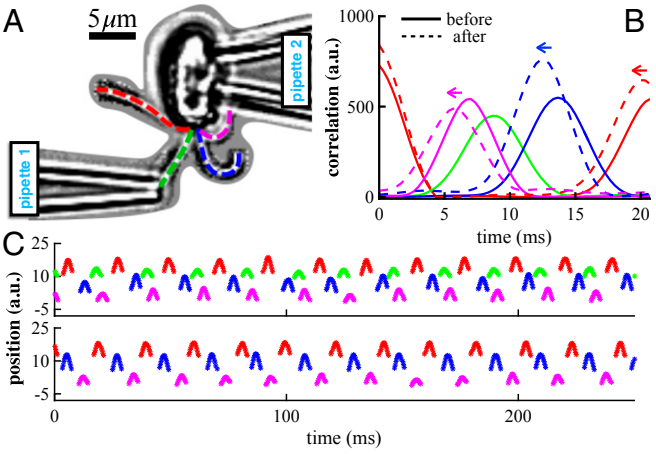

Fig. 4. (*A*) Stalling the flagellum beat in *T. suecica*. (*B*) Beat correlations for each flagellum relative to a reference flagellum (red) computed before and after manipulation shows period shift but no change in the order of flagella actuation. (*C*) Timeseries or footprints delineate positions of flagella (labeled as in *A*) before (*Top*) and after (*Bottom*) manipulation.

as scales and theca), have served as key diagnostics for mapping the likely phylogenetic relationships existing between species (42, 43).

We selected unicellular species of evolutionary interest to exemplify configurations of 2, 4, 8, or even 16 flagella (Movies S5–S8). These include (Fig. 5) distinct genera of biflagellates and quadriflagellates, both occurring abundantly in nature, the rare octoflagellate marine Prasinophyte known as *Pyramimonas octopus*, and its relative *Pyramimonas cyrtoptera*—the only species known with 16 flagella (44). Indeed, only three *Pyramimonas* species have eight flagella during all or parts of their cell cycles (45–47). Several species belong to the Prasinophytes—a polyphyletic class united through lack of similarity with either of the main clades (Chlorophyta and Streptophyta), whose >16 genera and >160 species (48) display a remarkable variability in flagella number and arrangement that is ideal for the present study.

Distinct quadriflagellate gaits were identified, involving particular phase relations between flagella. An analogy may be drawn with quadruped locomotion (Figs. 5 and 6). For measured flagellar phases ψ_j (flagellum index j), we compute the matrix $\Delta_{ij} = \psi_i - \psi_j$ $(i,j = 1, \ldots, 4)$, where $\Delta_{ij} = \Delta_{ji}$, $\Delta_{ii} = 0$, and $\Delta_{ik} = \Delta_{ij} + \Delta_{jk}$. Each gait is then associated with a 3-tuple of phase differences: $[\Delta_{12}\ \Delta_{13}\ \Delta_{14}]$. For instance, *Pyramimomas parkeae* swims with two pairs of precisely alternating breaststrokes akin to the "trot" of a horse (Fig. 6*A* and Movie S6); its four isokont flagella insert anteriorly into an apical pit, emerging in a cruciate arrangement typical of quadriflagellates (Fig. 6, type I). The phase relation $[\Delta_{12}\ \Delta_{13}\ \Delta_{14}] = [\pi\ 0\ \pi]$ is seen in both free-swimming and micropipette-held cells. A Chlorophyte alga *Polytomella* sp. *parva* (Fig. 5) was also found to display this gait. Two further gaits (Movie S6) occur in the type *Pyramimonas* species *P. tetrarhynchus* (49), a freshwater alga. The first we term the "pronk," where all flagella synchronize with zero phase difference (Fig. 6*B*). In the second, flagella beat in a sequence typical of the transverse gallop in quadrupeds (Fig. 5). *P. tetrarhynchus* swims preferentially with the latter gait, whereas pronking can occur when the cell navigates near walls/obstacles, or when changing direction. The rotary gallop, with flagella beating counterclockwise (CCW) in orderly sequence (Fig. 6*C* and Movie S6) occurs in the volvocale *Carteria crucifera*. Finally, in *Tetraselmis* (recall Fig. 4), the flagella separate distally into pairs (Fig. 6, type II). Cells display the transverse gallop when free-swimming or pipette-held despite strong hydrodynamic interactions within each pair. An alternate synchronous gait of four flagella has been reported in this species (50), but was not observed under our experimental conditions.

Ordinarily, motive gaits whereby the limbs of a quadruped or arthropod are actuated in precise patterns are produced by networks of coupled oscillators controlled by a central pattern generator (CPG) or equivalent (51, 52). Analogously, can we relate symmetries of the flagellar apparatus to gait symmetries, with contractile filaments providing the putative coupling? We focus on quadriflagellates, where an abundance of species makes possible comparative study (Fig. 6). Spatial symmetries of flagella $\mathbf{X}_j$ (indexed by

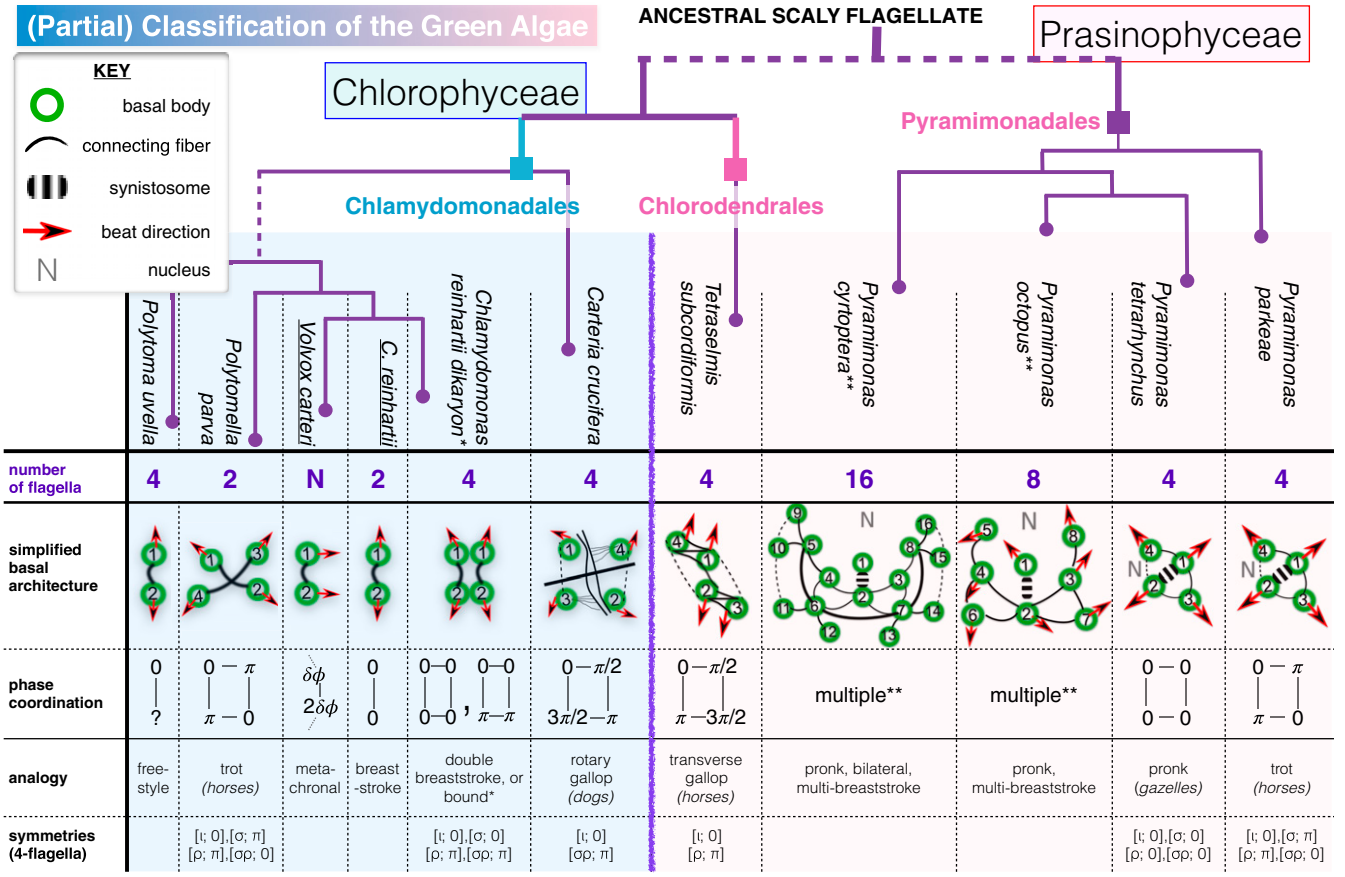

Fig. 5. Algal species are compared in terms of phylogeny, number and orientation of flagella, arrangement of BBs/basal architecture (see also *SI Appendix*), and patterns of coordination defined by the relative phases between flagella. Vertical lines approximate the relative phylogenetic distance from a putative flagellate ancestor (*SI Appendix*) (only partial branchings are shown). Free-swimming quadriflagellate gaits are readily identified with quadruped locomotion, revealing the symmetries of an underlying oscillator network. Asterisk (*): Quadriflagellate dikaryons of CR gametes perform a double breaststroke gait with the same symmetries as the pronk (Movie S5), but this gives way to a bound gait when both sets of flagella undergo phase slips simultaneously. Double asterisk (**): See Movies S7 and S8.

$j = 1,2,3,4$) are represented as permutations σ of $\{1,2,3,4\}$, so that $\mathbf{X}_k(t) = \mathbf{X}_{\sigma(k)}(t)$ for all times t. Periodic gaits also possess temporal symmetries: If T is the gait period, then, for the kth oscillator, $\mathbf{X}_k(t) = \mathbf{X}_k(t+T)$ for all t. We normalize T to 2π and consider invariance of flagella under phase shifts ϕ taken modulo $T/2\pi$; the pair $[\sigma, \phi]$ denotes a spatial–temporal symmetry of the $\{\mathbf{X}_j\}$, where

$$\mathbf{X}_k(t) = \mathbf{X}_{\sigma(k)}(t-\phi), \qquad [2]$$

and $k = 1, \cdots, 4$. The set of spatiotemporal symmetries may admit a (symmetry) group under composition,

$$[\sigma_1; \phi_1] \circ [\sigma_2; \phi_2] = [\sigma_1\sigma_2; \phi_1 + \phi_2], \qquad [3]$$

to be matched with known quadruped/quadriflagellate gaits. For a basal morphology of a rectangularly symmetric network (51) with distinct lengthwise and crosswise couplings—in Fig. 5 (phase coordination) represented by lines of differing lengths—spatial symmetries include ι (the identity, fix everything), $\sigma = (12)(34)$ (reflect in y axis), $\rho = (13)(24)$ (reflect in x axis), and $\sigma\rho = (14)(23)$ (interchange of diagonals). In Fig. 5, we attach named gaits and associated symmetry groups to the species in which they are observed. Additionally, some quadriflagellates display a "stand" gait (a transient rest phase where no flagellum beats); this has the largest number of symmetries: $[\iota; \phi]$, $[\sigma; \phi]$, $[\rho; \phi]$, $[\sigma\rho; \phi]$, for arbitrary ϕ.

Can such a network resemble coupling of algal flagella? Despite significant variation across species, linkages or roots connecting BBs are key systematic characters. These can be microtubular or fibrillar. Microtubular roots, which were probably asymmetric in very early flagellates (20), position BBs and attached flagella during development (two per BB: termed left, right). The right root is generally two-stranded, and, together with the left root (X-stranded), forms an X-2-X-2 cruciate system characteristic of advanced green algae [$X = 4$ in CR (18)]. Only one absolute configuration of BBs exists for each species, and its mirror-symmetric form is not possible (53). For instance, in CR, two BBs emerge at 70–90° with a clockwise (CW) offset characteristic of advanced biflagellate algae (Fig. 1*D*); in contrast, many evolutionarily more primitive flagellates have BBs oriented with a CCW offset (20). Fibrillar roots, classified as system I or II (43), become more numerous with flagella number. These are generally contractile, likely contributing to interflagellar coupling. Each BB is unique up to the imbrication of its member tubules: A constant positional relationship pertains between its two roots and a principal connecting fiber linking the two ontogenetically oldest BBs, labeled 1,2 in keeping with convention (53, 54). It is this fiber that is mutated in *vfl3* mutants (recall Fig. 2).

Take a quadriflagellate species for which the basal architecture is known, and consider its associated swimming mode. In *P. parkeae* (Fig. 6*A*), a prominent (striated) DF called the synistosome links BBs 1,2 only (55), so that the coupling is different between different pairs. In the advanced heterotroph *Polytomella parva*, which swims with a comparable gait, flagella form opposing V-shaped pairs with different coupling between pairs (56). In *Tetraselmis*, the flagella separate distally into two nearly collinear pairs with BBs forming a single zig-zag array (Fig. 5), in a state thought to have arisen from rotation of two of the flagellar roots in an ancestral quadriflagellate. Transfibers that are functionally related to the *Chlamydomonad* PF and DF connect alternate BBs, whereas BBs within the same pair are linked by Z-shaped struts (57), emphasizing a diagonal connectivity that may explain its transverse gallop (Fig. 6*D*). In contrast, the rotary gallop, prominent in *C. crucifera* (Fig. 6*C*), is more consistent with a square symmetric network involving near-identical connectivity between neighboring flagella than with a rectangular one. Indeed, the flagellar apparatus in this species has been shown to exhibit unusual rotational symmetry: BBs insert into an anterior papilla at the corners of a square in a cruciate pattern [class II *sensu* Lembi (58)] and are tilted unidirectionally in contrast to the conventional V shapes found in *Chlamydomonas* and *Polytomella*. [Here DFs, rather than linking directly to BBs, attach to rigid electron-dense rods extending between them (58).] Finally, a different network of couplings appears when two biflagellate CR gametes fuse during sexual reproduction (59) to form a transiently quadriflagellate dikaryon (similar to configuration II, Fig. 6). Here, original DFs between *cis* and *trans* remain, but new fibers do not form between pairs of flagella of unlike mating type. Strong hydrodynamic coupling due to their physical proximity results in a striking double bilateral breaststroke (Movie S5). A "bound"-like gait can appear if both sets of CR flagella slip together (Fig. 5).

Thus, algal motility appears to be constrained by the form of underlying coupling provided by a species-specific configuration of BBs and connecting fibers. The case of octoflagellates and hexadecaflagellates swimming is more complex (Movies S7 and S8),

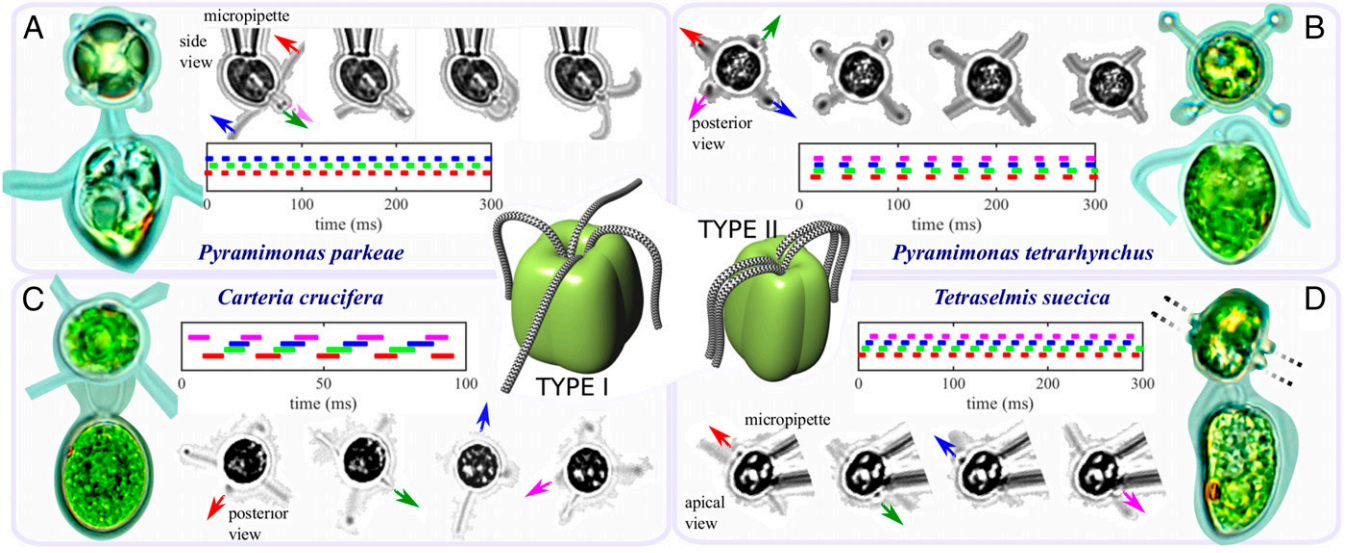

Fig. 6. In free-living quadriflagellates, flagella can be arranged in one of two possible configurations (types I, II)—type II is unusual. Gaits of coordination are diverse and species-specific, including the trot (*A*), pronk (*B*), rotary (*C*), and transverse (*D*) gallops. Representative species, imaged from top and side, show locations of eyespots and chloroplast structures. Timeseries of phases are measured for pipette-held cells in *A* and *D* and free-swimming cells in *B* and *C*.

limited by the number of species available for study, and presence of a large number of fibrous structures whose identities remain unknown. A consistent numbering system for BBs has greatly facilitated the study of flagellar transformation in algae with many flagella, which we adopt (53, 54). As in other *Pyramimonas*, BBs 1,2 remain connected by a large synistosome (Fig. 5). In *P. octopus*, up to 60 individual fibers establish specific connections with specific BB triplets, in addition to six to eight rhizoplasts linking the basal apparatus to the nucleus. Numerous rhizoplasts and connecting fibers also exist in *P. cyrtoptera* but were never resolved fully because of the untimely death of T. Hori (60). In *P. octopus* (Fig. 7), BBs arrange in a diamond (partially open to allow nuclear migration during mitosis). BB duplication is semiconservative (61): Eight new BBs form peripheral to the existing ones during cell division (54). The innermost BBs (1,2) assume the new position 1 in the two daughters (i.e., full maturation) after round 1 of cell division, but BBs 3,4 and 5–8 only reach maturation after rounds 2, 3, respectively (47, 54). All 2^n BBs in a given cell reach and thereafter remain at position 1 by the nth generation [see *P. cyrtoptera* (44)].

In electron micrographs of *P. octopus*, flagellar beating is oriented in CCW sequence (47, 54) consistent with observed CW body rotation (viewed from above). Cells ≈20 μm in length, with yet longer flagella whose distal portions fold and recurve by the cell, swim at ∼200–300 μm/s along helical paths. Diametrically opposite groups (usually but not exclusively pairs) of flagella beat synchronously with ordered phase shifts between groups (Fig. 7*A* and Movie S7). IP coupling appears more robust in distinguished pairs (Movie S7), reflecting prominent symmetries of the basal architecture; e.g., a large synistosome links BBs 1,2, whose flagella beat in opposite directions (Fig. 5). Compatible with its benthic nature, *P. octopus* display the stand gait introduced previously (Fig. 7*B*). Swimming motion resumes spontaneously when all eight flagella reactivate (pronking), and the normal gait is reestablished within only two or three beats. A transient state in which beating occurs in four of eight flagella (staggered) is observed in Fig. 7*D*, in which actively beating flagella are identified by summing successive gradient images (in contrast, in Fig. 7*C*, all eight flagella are in motion). We visualize the flow disturbance imparted by flagellar beating using optical flow to monitor the migration of image pixels between frames, and estimate flow directions and magnitudes (62) (also Computer Vision toolbox, MATLAB; The MathWorks, Inc.). Components of the 2D flow field were determined by minimizing an objective function subject to certain global (smoothness) or local (fidelity) constraints, and pixels delineating the same object are likely to have constant intensity. Unlike conventional particle image velocimetry (PIV) methods, this removes the need to seed the medium with foreign particles or tracers, and fluid flow due to motion can be obtained directly from optical data. Flow strengths decay rapidly away from boundaries of flagella as well as the cell body, which is also in motion (Fig. 7 *C* and *D*, *Right*). More generally, gait transitions in these primitive algae can be dramatic and involve unusual flagellar coordination in response to external stimuli. Here, we reserve special attention to the *P. cyrtoptera* pronking gait, which displays striking hydrodynamic interactions.

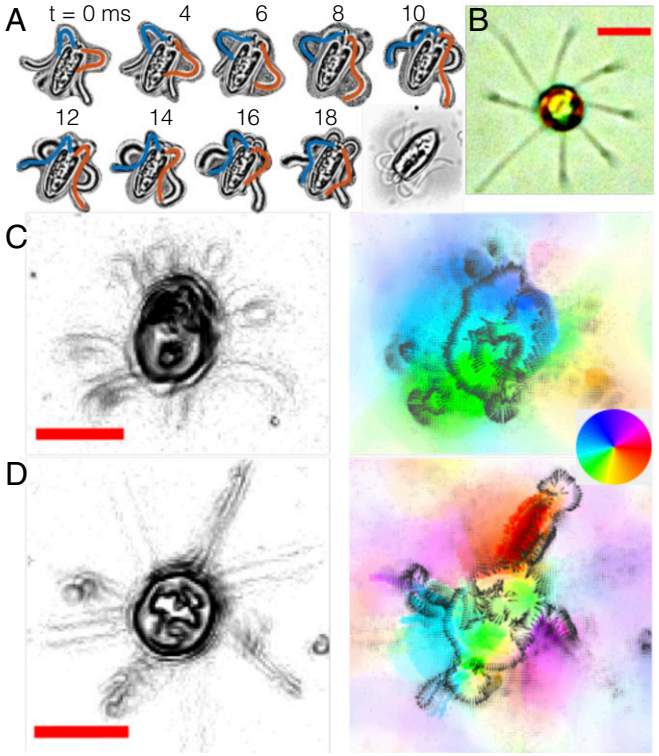

Fig. 7. *P. octopus* cell (*A*) swims using multiple pairs of breaststrokes: highlighted are waveforms of one synchronous pair. In *B*, cell is at rest in a stand gait in which no flagellum is active. (*C* and *D*) Gradient images (*Left*) identify the active subset of flagella (all in *C*, or four of eight in *D*); optical flow fields (*Right*) show decay of beating-induced flow disturbance. (Scale bar: 10 μm.)

Hydrodynamic Synchronization in a Hexadecaflagellate. *P. cyrtoptera* is the only hexadecaflagellate known (63). It is an Arctic species thought to have evolved when *P. octopus* failed to divide after duplication of chloroplasts and flagella. Measuring up to 40 μm, this is the largest *Pyramimonas* ever recorded. Its 16 flagella (32 when dividing), which are longer than the cell and emerge radially from a deep anterior flagellar pit (Fig. 8 *A* and *B*), are used by the organism to attach to icy surfaces. The name *P. cyrtoptera* is derived from the Greek for *cyrtos*, meaning "curved," and *pteron*, meaning "wing," in reference to cell morphology. Light microscopy reveals a lobed structure with two pairs of split eyespots and the presence of two chloroplasts (Fig. 8*C*). *P. cyrtoptera* cells are stenothermal and euryhaline: Growth becomes limited above 7–8 °C. Once removed from their natural habitat where temperature variations are typically <2 °C, cell cultures often prove fragile and difficult to maintain in the laboratory.

Hexadecaflagellate swimming presents an intriguing circumstance in which the distance of separation between flagella is so small that hydrodynamic coupling is inevitable. When fully splayed (Fig. 8*B*), the 16 flagella are separated, on average, by $360/16 = 22.5°$ or 7.85 μm measured at a radial distance of 20 μm from the cell, compared with $360/8 = 45°$ and twice this distance in *P. octopus*. In *P. cyrtoptera*, the interflagellar distance is thus far below the critical length to achieve synchronization by hydrodynamics (12). Strong hydrodynamic interactions are evident between some or even all flagella (Movie S8), none more so than during the pronk. Instead of tracking individual flagella (which beat in synchrony), we use the area $\mathcal{A}(t)$ bounding the flagella as proxy for phase of beat cycle (normalized),

$$\phi_{16}(t) = \left(\frac{t - t_n}{t_{n+1} - t_n}\right) \quad [t_n \le t \le t_{n+1}], \qquad [4]$$

where t_n are discrete marker events corresponding to local maxima of $\mathcal{A}(t)$. Pronking occurs at ∼25 Hz (Fig. 8*D*). Significant hydrodynamic effects are also evidenced in cells swimming against surfaces, where flagella exhibit symplectic metachronal waves (*SI Appendix*).

Discussion

Insufficiency of Hydrodynamics. The phenomenon of cooperative or synchronous beating of cilia and flagella has received growing attention, with hydrodynamic interactions historically assumed to be the major source of coupling. It is only recently (15, 31, 32) that researchers have begun to question this long-standing belief. Our approach was motivated in part by the freestyle gait (AP) in the CR

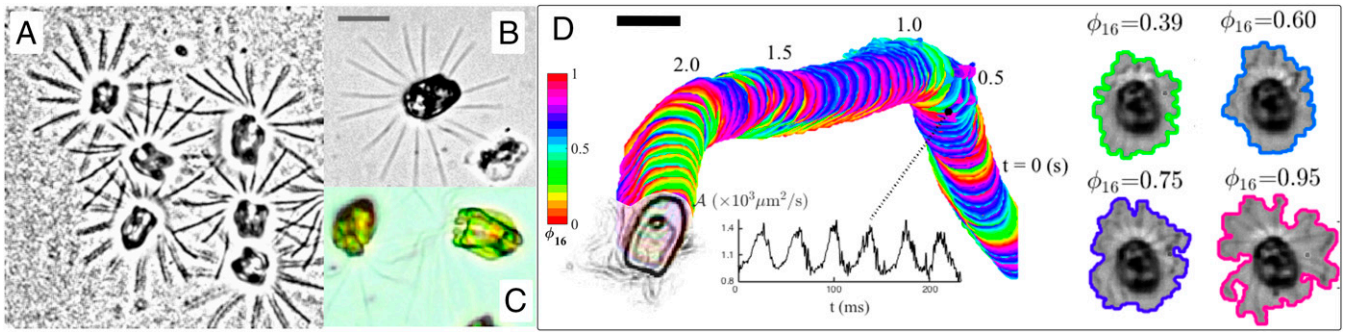

Fig. 8. In the rare Arctic species *P. cyrtoptera*, flagella can remain at rest for seconds in a stand gait (*A* and *B*). One such cell, where all 16 flagella are visible, is shown in *B*. Cells appear yellow-green and lobed (*C*). (*D*) Pronking involving all 16 flagella (Movie S8) is a common swimming gait. The cell body is tracked along a typical trajectory and colored by normalized phase ϕ_{16} (colorbar), computed from the area $\mathcal{A}(t)$ bounding the flagella that expands and contracts according to the periodicity of flagellar beating (shown here at four representative phases). (*Inset*) Time series of $\mathcal{A}$ over six successive cycles. (Scale bar: 20 μm.)

phototaxis mutant *ptx1*, realizing that the wild-type IP breaststroke cannot be reconciled with hydrodynamic theory (15, 16). An additional ingredient, internal to the cell, must be maintaining IP synchrony in CR. The finding that entrainment of CR flagella by periodic external flows only occurs at frequencies close to the natural beat frequency and strengths greatly in excess of physiological values led Quaranta et al. to a similar conclusion (32). The DF likely couples CR flagella, providing a degree of freedom that can reorient a flagellum at the BB through its contraction. In isolated and reactivated flagella apparatuses, for example, the DF constricts in response to elevated extracellular calcium to reduce the opening angle between the two BBs (35). Because BBs nucleate/anchor flagella and function as centrioles during cell division, the DF can also be affected by mutations in BB duplication and segregation (36). This brings us back to the unusual flagellar coordination in *ptx1*, which is thought to possess two *trans*-like flagella (64). If BB signaling or connectivity is disrupted or weakened in *ptx1*, stochastic IP/AP transitions can result when hydrodynamic interactions compete with a reduced intracellular coupling (15). Indeed, for all their DF defects, flagella of *vfl3* do not synchronize, or only hydrodynamically, when very close together (Fig. 2). Future work should seek to examine flagellar apparatuses of *ptx1* under electron microscopy. The failure of hydrodynamics to synchronize two flagella in a CR-like configuration, let alone two functionally distinct flagella such as a *cis* and a *trans* (16, 65), was shown by micromanipulation of two pipette-held cells (Fig. 2).

The diversity of coordination gaits in flagellate species (Fig. 5) implicates internal coupling as a generic remedy for this insufficiency of hydrodynamics. Indeed, nonuniqueness of stable quadriflagellate gaits for even identical configurations of four flagella is incompatible with the existence of a single hydrodynamic mode. In some species, a number of gait bifurcations can occur during free-swimming, involving modification or even cessation of beating in one or more flagella, suggesting coordination is an active process. The significant perturbation to the hydrodynamic landscape resulting from immobilizing one flagellum in *Tetraselmis suecica* was found to have little effect on the native coordination of the remainder (Fig. 4). Thus, symmetries of flagellar gaits are much more species- than drag-dependent.

Intracellular Coupling of Flagella by Contractile Fibers. Gaits are defined by the relative phase between oscillators, which, in the analogy of multilegged locomotion, may be produced by CPG or pacemaker signals, which, in algae, we conjecture to be mediated by the basal architecture. Flagellar apparatuses imaged by electron microscopy reveal species-specific networks of connections that increase in complexity with flagella number (19). Symmetries of an underlying network of structural couplings (51) likely translate downstream into symmetries of observed multiflagellate gaits (Fig. 5). The BB from which the flagellum nucleates is a center for conduction of morphogenetic and sensory information between flagella and other intracellular organelles. Although BBs are not essential for flagellar function [isolated axonemes continue to beat when reactivated in ATP (66, 67)], the contractility of inter-BB connections may contribute to coordination (68). In CR, robust NBBCs descending near the DF link BBs to the nucleus (Fig. 1*B*), and remain intact even after detergent lysis treatment (37). These can be induced by calcium to undergo significant contraction (69). Similarly, rhizoplasts of scaly algae, including *Pyramimonas* and *Tetraselmis*, can contract and relax cyclically (43, 50). These species display frequent directional changes (mechanoshock) that may be mediated by the extraordinary contractility of rhizoplasts (50), with normal coordination after abrupt gait changes rapidly reestablished. Fibrillar structures under tension experience much distortion during active beating, as observed from misalignment of fiber striation patterns (70). Contraction during live beating is ATP-dependent in *Polytomella* (71), occurs in real time in paralyzed flagella and temperature-sensitive mutants of *Chlamydomonas* (72), and occurs to an extraordinary degree in *Microthamnion* zoospores (73). ATPase activity has also been identified in the rod cells of the human eye where a large striated root attaches to the BB of a short (nonmotile) cilium (74). Attachment sites of contractile fibers also exhibit great specificity, in most species to specific microtubule triplets and disk complexes. In *P. octopus*, contractile fibers attach to the "weaker" side of BBs (triplets 6–9), and may function to pull the flagellum back from each power stroke during its unique multibreaststroke gait.

Evolution of Multiflagellation Among Viridiplantae. As an appendage, cilia, flagella, and its $9+2$ axoneme prevails across eukaryotes and, especially, the green algae. Yet, beyond the universality of this basic machinery, much variability (Fig. 5) persists in the placement of organelles, form of flagellar insertion, and diversity of flagellar coordination. The basal apparatus is that rare structure that is both universally distributed and stable enough to infer homology across large phylogenetic distances, and yet variable enough to distinguish between different lineages. Representative species considered here express 2^n flagella, with much conservatism in the biflagellate or quadriflagellate condition. Since an early flagellate phagocytosed a prokaryote (the future chloroplast) >1 billion years ago, green algae have evolved photosynthesis and autotrophism (75). Their radiation and division into the Streptophyta and Chlorophyta (76) has been corroborated by modern high-throughput chloroplast genome sequencing (77). Occupying a basal phylogenetic position are morphologically diverse species of freshwater and marine *Prasinophytes*, including the *Pyramimonas* species (20) studied here. These have conspicuous body and flagella scales that are precursors of theca and volvocalean cell walls (53). In particular, *P. tetrarhynchus*, *P. octopus*, and *P. cyrtoptera* are assigned according to morphological characters (78) to the same subgenus, in which accelerated rates of evolution

were confirmed by cladistic analysis of *rbcL* gene sequences (Fig. 5). Changes in basal ultrastructure were major events (20), with the quadriflagellate condition arising multiple times; in fact, it is the quadriflagellates (e.g., *Carteria*) and not Chlamydomonad-type biflagellates that are considered basal to advanced volvocales (77, 79). The advanced heterotrophic alga *Polytomella*, thought to have evolved by cell doubling along a direct line of descent from CR (80), displays the same trot gait as the ancestral *P. parkeae*. In these cases, convergent ultrastructural modifications coincident with multiplicity and doubling of BBs may have evolved to enable strong coupling between opposite flagella pairs.

The sparsity of species bearing >4 localized flagella (*P. octopus*, *P. cyrtoptera*) may stem from the difficulty and activity costs of a flagellar apparatus capable of maintaining coordination from within despite external effects such as hydrodynamics. *P. cyrtoptera* exemplifies an intermediate between few to many flagella [16 is the highest number ever reported in a phytoflagellate (44)], and is able to exploit hydrodynamics for swimming in a novel manner (Fig. 5). The energetic gains of such cooperativity may have inspired derivation of multiflagellated colonial volvocales from unicellular ancestors. Opportunities for fluid-mediated flagellar coordination and metachronism impose new constraints on the configuration of flagella and BBs. In VC somatic cells, for example, BBs reorient during early stages of development to become parallel (Fig. 1*C*), whereas biflagellate VC sperm cells (required to swim independently) retain the primitive V formation.

Implications for Active Control of Flagellar Coordination. From the comparative studies carried out in this work, we conclude that the physical principle for coordinating collective ciliary beating in *Volvox* or *Paramecium* differs from that responsible for defining precise patterns of beating in unicellular microswimmers bearing only a few flagella. In the former case, hydrodynamic coupling between flagella is sufficient (12), but, in the latter (especially for obligate autotrophs), there is far greater incentive for efficient swimming to be robust despite hydrodynamic perturbations. Even in arrays of mammalian cilia, ciliary roots and basal feet structures continue to provide additional resistance to fluid stresses (22, 81).

Rapid changes in cellular structure that are of fundamental evolutionary interest may have arisen, in the first instance, in green flagellates than higher organisms. At the base of flagella in these algae are found diverse networks of interconnecting filaments that are not only responsible for anchorage and placement of flagella but that must now also be implicated in defining the symmetries of flagellar coordination. In CR, for instance, most BB connections do not appear until after the BBs have already formed. Fiber contractility can produce elastic coupling between BBs to force nearby flagella into modes of synchrony (IP or AP) that oppose hydrodynamic influences (15, 82). This elasticity may be actively modulated, highlighting a direct correlation between cellular physiology and flagellar beating that has already been identified (27, 83). Further insights into such processes will certainly require additional modeling and experimentation. The rapidity with which patterns of synchrony can change is suggestive of transduction by electrical signals or ionic currents (84), which may be effected from cell interior to flagella by changes in the state of contraction or relaxation of connecting fibers. Striations of algal rhizoplasts are even biochemically mutable in a manner reminiscent of mammalian muscle. We are therefore led to suggest that a parallel evolution of neuromuscular control of appendages may have occurred much earlier than previously thought (50, 85).

Materials and Methods

Culturing and Growth of Algae. Below are brief descriptions of the protocols for species whose flagellar dynamics are studied here.

Volvox. *V. carteri* was prepared as described elsewhere (12). The remaining species, unless otherwise specified, were maintained under controlled illumination on 14-h day/10-h night cycles, and at a constant temperature of 22 °C (incubation chamber; Binder).

Pyramimonas. Marine species obtained from the Scandanavian Culture Collection of Algae and Protozoa, K-0006 *P. parkeae* R.E. Norris et B.R. Pearson 1975 (subgenus *Trichocystis*), K-0001 *P. octopus* Moestrup et Aa. Kristiansen 1987 (subgenus *Pyramimonas*), and K-0382 *P. cyrtoptera* Daugbjerg 1992 (subgenus *Pyramimonas*), were cultured in TL30 medium (www.sccap.dk/media/). Of these, *P. cyrtoptera* is an Arctic species and was cultured at 4 °C. A fourth *Pyramimonas*, K-0002 *P. tetrarhynchus* Schmarda 1850 (type species), is a freshwater species, and was grown in enriched soil medium NF2 (www.sccap.dk/media/).

Tetraselmis. Marine species *T. suecica* (gift from University of Cambridge Department of Plant Sciences) and *Tetraselmis subcordiformis* (CCAP 116/1A), were cultured in the f/2 medium (www.ccap.ac.uk/pdfrecipes.htm).

Polytoma. *Polytoma uvella* Ehrenberg 1832 (CCAP 62/2A) was grown in *Polytoma* medium [comprising 2% (wt/vol) sodium acetate trihydrate, 1% yeast extract, and 1% bacterial tryptone (www.ccap.ac.uk/pdfrecipes.htm)].

Polytomella. Two species (CCAP 63/1 and CCAP 63/3) were maintained on a biphasic soil/water medium (www.ccap.ac.uk/pdfrecipes.htm).

Carteria. *C. crucifera* Korschikov ex Pascher (1927) from CCAP (8/7C) was grown in a modified Bold basal medium (www.ccap.ac.uk/pdfrecipes.htm).

Chlamydomonas. *C. reinhardtii* strains were obtained from the Chlamydomonas Collection, wild-type CC125, and variable flagella mutant *vfl3* (CC1686), and grown photoautotrophically in liquid culture [tris-acetate phosphate (TAP)].

Production of quadriflagellate dikaryons. High-mating efficiency strains of *C. reinhardtii* CC620 (mt^+), CC621 (mt^-) were obtained from the Chlamydomonas Collection and grown photoautotrophically in nitrogen-free TAP to induce formation of motile gametic cells of both mating types. Fusing of gametes occurred under constant white light illumination.

Manipulation of Viscosity. To facilitate identification of flagella in certain species, the viscosity of the medium was increased by addition of methyl cellulose (M7027, 15 cP; Sigma-Aldrich) to slow down cell rotation and translation rates.

Microscopy and Micromanipulation. The capture of single cells is as described elsewhere (12, 14, 16, 27). For Fig. 3*A*, caught CR cells were examined under the light microscope to identify the eyespot and thus *cis* and *trans* flagella; the correct flagellum was then carefully removed using a second pipette with smaller inner diameter.

ACKNOWLEDGMENTS. We thank Kyriacos Leptos and Marco Polin for discussions relating to the contractility of the basal apparatus at an early stage of this work, and the possible insights provided by the *vfl* class of mutants; François Peaudecerf for kindly providing the CR gametes; and Matthew Herron, Thomas Pröschold, and Stephanie Höhn for valuable comments on the manuscript. This work is supported by a Junior Research Fellowship from Magdalene College Cambridge (to K.Y.W.) and a Wellcome Trust Senior Investigator Award (to R.E.G.).

1. Machemer H (1972) Ciliary activity and the origin of metachrony in Paramecium: Effects of increased viscosity. *J Exp Biol* 57(1):239–259.
2. Goldstein RE (2015) Green algae as model organisms for biological fluid dynamics. *Annu Rev Fluid Mech* 47:343–375.
3. Orme BAA, Otto SR, Blake JR (2001) Enhanced efficiency of feeding and mixing due to chaotic flow patterns around choanoflagellates. *IMA J Math Appl Med Biol* 18(3):293–325.
4. Kramer-Zucker AG, et al. (2005) Cilia-driven fluid flow in the zebrafish pronephros, brain and Kupffer's vesicle is required for normal organogenesis. *Development* 132(8):1907–1921.
5. Guirao B, Joanny JF (2007) Spontaneous creation of macroscopic flow and metachronal waves in an array of cilia. *Biophys J* 92(6):1900–1917.
6. Lechtreck KF, Sanderson MJ, Witman GB (2009) High-speed digital imaging of ependymal cilia in the murine brain. *Methods Cell Biol* 91:255–264.
7. Smith DJ, Gaffney EA, Blake JR (2008) Modelling mucociliary clearance. *Respir Physiol Neurobiol* 163(1-3):178–188.
8. Gray J (1928) *Ciliary Movement* (Cambridge Univ Press, Cambridge, UK).
9. Rothschild (1949) Measurement of sperm activity before artificial insemination. *Nature* 163(4140):358–359.
10. Riedel IH, Kruse K, Howard J (2005) A self-organized vortex array of hydrodynamically entrained sperm cells. *Science* 309(5732):300–303.
11. Gueron S, Levit-Gurevich K (1999) Energetic considerations of ciliary beating and the advantage of metachronal coordination. *Proc Natl Acad Sci USA* 96(22):12240–12245.
12. Brumley DR, Wan KY, Polin M, Goldstein RE (2014) Flagellar synchronization through direct hydrodynamic interactions. *eLife* 3:e02750.
13. Solari CA, et al. (2011) Flagellar phenotypic plasticity in volvocalean algae correlates with Péclet number. *J R Soc Interface* 8(63):1409–1417.

14. Brumley DR, Polin M, Pedley TJ, Goldstein RE (2012) Hydrodynamic synchronization and metachronal waves on the surface of the colonial alga *Volvox carteri*. *Phys Rev Lett* 109(26):268102.
15. Leptos KC, et al. (2013) Antiphase synchronization in a flagellar-dominance mutant of *Chlamydomonas*. *Phys Rev Lett* 111(15):158101.
16. Wan KY, Leptos KC, Goldstein RE (2014) Lag, lock, sync, slip: The many 'phases' of coupled flagella. *J R Soc Interface* 11(94):20131160.
17. Huygens C (1673) *Horologium Oscillatorium, Sive, de Motu Pendulorum ad Horologia Aptato Demostrationes Geometricae* (F. Muguet, Paris).
18. Ringo DL (1967) Flagellar motion and fine structure of the flagellar apparatus in *Chlamydomonas*. *J Cell Biol* 33(3):543–571.
19. Inouye I (1993) Flagella and flagellar apparatuses of algae. *Ultrastructure of Microalgae*, ed Berner T (CRC, Boca Raton, FL), pp 99–133.
20. Irvine D, John D, eds (1984) *Systematics of the Green Algae,* Systematics Association Special Volume (Academic, New York), Vol 27.
21. Kunimoto K, et al. (2012) Coordinated ciliary beating requires *Odf2*-mediated polarization of basal bodies via basal feet. *Cell* 148(1-2):189–200.
22. Galati DF, et al. (2014) DisAp-dependent striated fiber elongation is required to organize ciliary arrays. *J Cell Biol* 207(6):705–715.
23. McFadden GI, Schulze D, Surek B, Salisbury JL, Melkonian M (1987) Basal body reorientation mediated by a Ca^{2+}-modulated contractile protein. *J Cell Biol* 105(2): 903–912.
24. Carl C, de Nys R, Lawton RJ, Paul NA (2014) Methods for the induction of reproduction in a tropical species of filamentous ulva. *PLoS One* 9(5):e97396.
25. Gilbert FA (1927) On the occurrence of biflagellate swarm cells in certain myxomycetes. *Mycologia* 19(5):277–283.
26. Dieckmann CL (2003) Eyespot placement and assembly in the green alga *Chlamydomonas*. *BioEssays* 25(4):410–416.
27. Wan KY, Goldstein RE (2014) Rhythmicity, recurrence, and recovery of flagellar beating. *Phys Rev Lett* 113(23):238103.
28. Ruffer U, Nultsch W (1987) Comparison of the beating of *Cis*-flagella and *Trans*-flagella of *Chlamydomonas* cells held on micropipettes. *Cell Motil Cytoskeleton* 7(1): 87–93.
29. Goldstein RE, Polin M, Tuval I (2009) Noise and synchronization in pairs of beating eukaryotic flagella. *Phys Rev Lett* 103(16):168103.
30. Bruot N, Kotar J, de Lillo F, Cosentino Lagomarsino M, Cicuta P (2012) Driving potential and noise level determine the synchronization state of hydrodynamically coupled oscillators. *Phys Rev Lett* 109(16):164103.
31. Geyer VF, Jülicher F, Howard J, Friedrich BM (2013) Cell-body rocking is a dominant mechanism for flagellar synchronization in a swimming alga. *Proc Natl Acad Sci USA* 110(45):18058–18063.
32. Quaranta G, Aubin-Tam ME, Tam D (2015) On the role of hydrodynamics vs intracellular coupling in synchronization of eukaryotic flagella. *Phys Rev Lett* 115(23): 238101.
33. Witman GB (1993) *Chlamydomonas* phototaxis. *Trends Cell Biol* 3(11):403–408.
34. Lewin RA (1952) Studies on the flagella of algae. 1. general observations on *Chlamydomonas moewusii* Gerloff. *Biol Bull* 103(1):74–79.
35. Hyams JS, Borisy GG (1978) Isolated flagellar apparatus of *Chlamydomonas*: Characterization of forward swimming and alteration of waveform and reversal of motion by calcium ions in vitro. *J Cell Sci* 33(OCT):235–253.
36. Wright RL, Chojnacki B, Jarvik JW (1983) Abnormal basal-body number, location, and orientation in a striated fiber-defective mutant of *Chlamydomonas reinhardtii*. *J Cell Biol* 96(6):1697–1707.
37. Wright RL, Salisbury J, Jarvik JW (1985) A nucleus-basal body connector in *Chlamydomonas reinhardtii* that may function in basal body localization or segregation. *J Cell Biol* 101(5 Pt 1):1903–1912.
38. Geimer S, Melkonian M (2004) The ultrastructure of the *Chlamydomonas reinhardtii* basal apparatus: Identification of an early marker of radial asymmetry inherent in the basal body. *J Cell Sci* 117(Pt 13):2663–2674.
39. Hoops HJ, Wright RL, Jarvik JW, Witman GB (1984) Flagellar waveform and rotational orientation in a *Chlamydomonas* mutant lacking normal striated fibers. *J Cell Biol* 98(3):818–824.
40. Niedermayer T, Eckhardt B, Lenz P (2008) Synchronization, phase locking, and metachronal wave formation in ciliary chains. *Chaos* 18(3):037128.
41. Elfring GJ, Lauga E (2009) Hydrodynamic phase locking of swimming microorganisms. *Phys Rev Lett* 103(8):088101.
42. Stewart KD, Mattox KR (1978) Structural evolution in the flagellated cells of green algae and land plants. *Biosystems* 10(1-2):145–152.
43. Melkonian M (1980) Ultrastructural aspects of basal body associated fibrous structures in green algae: A critical review. *Biosystems* 12(1-2):85–104.
44. Daugbjerg N, Moestrup O (1992) Ultrastructure of *Pyramimonas cyrtoptera* sp.nov. (Prasinophyceae), a species with 16 flagella from northern Foxe basin, arctic Canada, including observations on growth rates. *Can J Bot* 70(6):1259–1273.
45. Conrad W (1939) Notes protistologique. xi. sur *Pyramidomonas amylifera* n. sp. *Bull Mus R Hist Nat Belg* 15:1–10.
46. Hargraves P, Gardiner W (1980) The life history of *Pyramimonas amylifera* Conrad (Prasinophyceae). *J Plankton Res* 2(2):99–108.
47. Hori T, Moestrup O (1987) Ultrastructure of the flagellar apparatus in *Pyramimonas octopus* (Prasinophyceae).1. Axoneme structure and numbering of peripheral doublets triplets. *Protoplasma* 138(2-3):137–148.
48. Sym SD, Piernaar RN (1991) Ultrastructure of *Pyramimonas norrisii* sp nov (Prasinophyceae). *Br Phycol J* 26(1):51–66.
49. Manton I (1968) Observations on the microanatomy of the type species of *Pyramimonas* (*P. tetrarhynchus* Schmarda). *Proc Linn Soc London* 179(2):147–152.
50. Salisbury JL, Floyd GL (1978) Calcium-induced contraction of the rhizoplast of a quadriflagellate green alga. *Science* 202(4371):975–977.
51. Collins JJ, Stewart IN (1993) Coupled nonlinear oscillators and the symmetries of animal gaits. *J Nonlinear Sci* 3(3):349–392.
52. Schöner G, Jiang WY, Kelso JAS (1990) A synergetic theory of quadrupedal gaits and gait transitions. *J Theor Biol* 142(3):359–391.
53. O'Kelly CJ, Floyd GL (1983-1984) Flagellar apparatus absolute orientations and the phylogeny of the green algae. *Biosystems* 16(3-4):227–251.
54. Moestrup O, Hori T (1989) Ultrastructure of the flagellar apparatus in *Pyramimonas octopus* (Prasinophyceae). 2. Flagellar roots, connecting fibers, and numbering of individual flagella in green-algae. *Protoplasma* 148(1):41–56.
55. Norris RE, Pearson BR (1975) Fine structure of *Pyramimonas parkeae* new species Chlorophyta Prasinophyceae. *Arch Protistenkd* 117(1-2):192–213.
56. Brown DL, Massalski A, Patenaude R (1976) Organization of the flagellar apparatus and associate cytoplasmic microtubules in the quadriflagellate alga *Polytomella agilis*. *J Cell Biol* 69(1):106–125.
57. Salisbury JL, Swanson JA, Floyd GL, Hall R, Maihle NJ (1981) Ultrastructure of the flagellar apparatus of the green alga *Tetraselmis subcordiformis* - with special consideration given to the function of the rhizoplast and rhizanchora. *Protoplasma* 107(1-2):1–11.
58. Lembi CA (1975) Fine-structure of flagellar apparatus of *Carteria*. *J Phycol* 11(1):1–9.
59. Harris EH (2009) *The Chlamydomonas Sourcebook*. *A Comprehensive Guide to Biology and Laboratory Use* (Academic, New York).
60. Hausman K, Radek R, eds (2014) *Cilia and Flagella—Ciliates and Flagellates: Ultrastructure and Cell Biology, Function and Systematics, Symbiosis and Biodiversity* (Schweizerbart Sci, Stuttgart, Germany).
61. Beech PL, Heimann K, Melkonian M (1991) Development of the flagellar apparatus during the cell cycle in unicellular algae. *Protoplasma* 164(1-3):23–37.
62. Sun D, Roth S, Black MJ (2014) A quantitative analysis of current practices in optical flow estimation and the principles behind them. *Int J Comput Vis* 106(2):115–137.
63. Daugbjerg N, Moestrup O, Archtander P (1994) Phylogeny of the genus *Pyramimonas* (Prasinophyceae, Chlorophyta) inferred from the *rbc*L gene. *J Phycol* 30(6):991–999.
64. Okita N, Isogai N, Hirono M, Kamiya R, Yoshimura K (2005) Phototactic activity in *Chlamydomonas* 'non-phototactic' mutants deficient in Ca^{2+}-dependent control of flagellar dominance or in inner-arm dynein. *J Cell Sci* 118(Pt 3):529–537.
65. Kamiya R, Witman GB (1984) Submicromolar levels of calcium control the balance of beating between the two flagella in demembranated models of *Chlamydomonas*. *J Cell Biol* 98(1):97–107.
66. Bessen M, Fay RB, Witman GB (1980) Calcium control of waveform in isolated flagellar axonemes of *Chlamydomonas*. *J Cell Biol* 86(2):446–455.
67. Mukundan V, Sartori P, Geyer VF, Jülicher F, Howard J (2014) Motor regulation results in distal forces that bend partially disintegrated *Chlamydomonas* axonemes into circular arcs. *Biophys J* 106(11):2434–2442.
68. Melkonian M (1983) Functional and phylogenetic aspects of the basal apparatus in algal cells. *J Submicrosc Cytol Pathol* 15(1):121–125.
69. Salisbury JL (1988) The lost neuromotor apparatus of *Chlamydomonas*: Rediscovered. *J Protozool* 35(4):574–577.
70. Gibbons IR, Grimstone AV (1960) On flagellar structure in certain flagellates. *J Biophys Biochem Cytol* 7(4):697–716.
71. White RB, Brown DL (1981) ATPase activities associated with the flagellar basal apparatus of *Polytomella*. *J Ultrastruct Res* 75(2):151–161.
72. Hayashi M, Yagi T, Yoshimura K, Kamiya R (1998) Real-time observation of Ca^{2+}-induced basal body reorientation in *Chlamydomonas*. *Cell Motil Cytoskeleton* 41(1):49–56.
73. Watson MW (1975) Flagellar apparatus, eyespot and behavior of *Microthamnion kuetzingianum* (Chlorophyceae) zoospores. *J Phycol* 11(4):439–448.
74. Matsusaka T (1967) ATPase activity in the ciliary rootlet of human retinal rods. *J Cell Biol* 33(1):203–208.
75. Cavalier-Smith T (1982) The origins of plastids. *Biol J Linn Soc London* 17(3):289–306.
76. Leliaert F, et al. (2012) Phylogeny and molecular evolution of the green algae. *Crit Rev Plant Sci* 31(1):1–46.
77. Buchheim MA, et al. (1996) Phylogeny of the Chlamydomonadales (Chlorophyceae): A comparison of ribosomal RNA gene sequences from the nucleus and the chloroplast. *Mol Phylogenet Evol* 5(2):391–402.
78. Mcfadden GI, Hill D, Wetherbee R (1986) A study of the genus *Pyramimonas* (Prasinophyceae) from southeastern Australia. *Nord J Bot* 6(2):209–234.
79. Nozaki H, Misumi O, Kuroiwa T (2003) Phylogeny of the quadriflagellate Volvocales (Chlorophyceae) based on chloroplast multigene sequences. *Mol Phylogenet Evol* 29(1):58–66.
80. Smith DR, Lee RW (2014) A plastid without a genome: Evidence from the nonphotosynthetic green algal genus *Polytomella*. *Plant Physiol* 164(4):1812–1819.
81. Brooks ER, Wallingford JB (2014) Multiciliated cells. *Curr Biol* 24(19):R973–R982.
82. Cosentino Lagomarsino M, Jona P, Bassetti B (2003) Metachronal waves for deterministic switching two-state oscillators with hydrodynamic interaction. *Phys Rev E Stat Nonlin Soft Matter Phys* 68(2 Pt 1):021908.
83. Ma R, Klindt GS, Riedel-Kruse IH, Jülicher F, Friedrich BM (2014) Active phase and amplitude fluctuations of flagellar beating. *Phys Rev Lett* 113(4):048101.
84. Harz H, Hegemann P (1991) Rhodopsin-regulated calcium currents in *Chlamydomonas*. *Nature* 351(6326):489–491.
85. Jékely G, Paps J, Nielsen C (2015) The phylogenetic position of ctenophores and the origin(s) of nervous systems. *Evodevo* 6:1.